IRON: an Integrated RF-OWC System for Interoperability in IoT Systems

Anna Maria Vegni*, Pietro Manzoni†, and Milica Petkovic‡

*Dept. of Industrial, Electronic and Mechanical Engineering, Roma Tre University, Italy. Email: annamaria.vegni@uniroma3.it

†Department of Computer Engineering, Universitat Politècnica de València, Spain. Email: pmanzoni@disca.upv.es

‡Faculty of Technical Sciences, University of Novi Sad, Serbia. Email: milica.petkovic@uns.ac.rs

***Abstract*—This paper presents IRON, an integrated Radio Frequency (RF)-Optical Wireless Communications (OWC) interoperability system for IoT deployments. Moving from traditional fully-RF IoT frameworks to a hybrid RF-OWC structure allows one to guarantee several benefits, from higher data rates to security enhancement, without increasing energy consumption. IRON framework exploits the visible light spectrum that can guarantee not only communications but also illumination at the same time, thus making it particularly useful in indoor scenarios. The interoperability between RF and OWC technologies occurs by means of control messages via the LoRa (Long Range) technology, that is able to reach longer distances even in indoor scenarios. The simulation results highlight the benefits of the IRON approach, expressed as the ability to meet specific data rate requirements with limited energy consumption.**

***Index Terms*—Internet of Things, interoperability, LoRa, Visible Light Communications.**

I. Introduction

In the rapidly evolving landscape of the Internet of Things (IoT), the need for diverse and robust communication technologies is paramount. Traditional IoT systems exploit the radio frequency (RF) spectrum but suffer from several drawbacks, such as electromagnetic compatibility in unique environments like hospitals or industrial settings [1].

Integrating RF technology with Optical Wireless Communications (OWC) can represent a viable solution for RF-based IoT systems. Indeed, OWC can be utilized in harsh environments to send and receive communication and sensor signals in a most effective and reliable way, thanks to higher data rates and wider bandwidth as compared to RF. Manie *et al.* [2] investigated the integration of laser-based OWC with a fiber sensor system for IoT applications. Larthani *et al.* [3] dealt with the use of lightwave technology like optical fiber, integrated into IoT systems for the detection of disasters such as floods, earthquakes, landslides, etc. A similar approach is presented by Margarat *et al.* [4], which investigated the use of an optical temperature sensor for usage in smart agriculture.

Recent advancements in IoT have enhanced monitoring technologies in both urban and rural areas, focusing on sensor-actuator interactions and high connectivity, especially in wireless systems. The challenge lies in achieving interoperability among diverse communication technologies. Various solutions have been provided that propose the integration and interoperability of various technologies, such as [5]–[8].

This paper delves into the synergistic potential of combining VLC, known for its high data rate capabilities in short-range communication, with LoRa, celebrated for its long-range and low-power consumption features. VLC, which utilizes the visible light spectrum for data transmission, offers a unique advantage in terms of bandwidth and security. It is inherently safe for human exposure and provides a vast, unregulated bandwidth immune to radio frequency interference. This makes VLC an ideal candidate for high-density, short-range communication scenarios often encountered in smart buildings, indoor navigation, and vehicle-to-vehicle communication. On the other hand, LoRa, a modulation technique derived from Chirp Spread Spectrum technology, is designed for long-range, low-power communication, making it a cornerstone in the IoT landscape. Its ability to cover extensive areas with minimal energy consumption and infrastructure makes it suitable for applications such as rural IoT connectivity, smart agriculture, and environmental monitoring.

In this paper, we present IRON, an integrated RF-OWC system for interoperability in IoT systems, aiming to explore the technical aspects of integrating VLC and LoRa, including the challenges and potential solutions in creating a seamless interface between these two technologies. We will examine use cases where this integration can provide significant advantages and that require high data throughput and extensive coverage.

This paper is organized as follows. Section II presents the proposed IRON architecture, comprised of a network of LoRa Relay Nodes (RNs) and several VLC indoor and outdoor subnetworks. Section III describes how IRON exchanges LoRa packets to coordinate and manage connectivity flows in VLC subsystem. This is defined by IRON pseudocode, where different procedures are presented. The simulation results showing the benefits of IRON framework to control the VLC data rate are collected in Section IV, comparing different VLC network deployments. Conclusions are drawn at the end of this paper.

II. IRON Architecture

IRON architecture is based on deploying hybrid LoRa-VLC nodes to control the end user requirements. The architecture is comprised of a VLC sub-system for both indoor and outdoor applications, overlapped by a LoRa layer with multiple RNs. In the VLC sub-system, various "islands" of connectivity are supposed to be in place, composed of various receiver nodes linked to one or many transmitter nodes. We are supposing that each island cannot interact through VLC with the other islands, thus improving communication security. The VLC monitoring and control is provided by LoRa RNs, which receive feedback information from the receiver nodes (*i.e.*, UEs) and forward control information to the VLC transmitters based on some rules that can be programmed in the controlling node.

LoRa-based communication is handled by AlLoRa [9], a modular, low-power, long-range communication protocol based on LoRa that allows one to interconnect using a dynamic and mesh-based architecture for all the integration nodes. In the following, we will use the term LoRa implying that this more robust version of the protocol is being used. The VLC nodes can adopt an OpenVLC [10] HW structure for example to establish the light-based links inside a cell.

Fig. 1 shows a schematic representation of three different network topologies or configurations involving hybrid LoRa and VLC nodes. Fig. 1(*a*) shows a linear topology for a point-to-point connectivity link from a LoRa source node (*i.e.*, LoRa GateWay) to a receiver photodetector (PD). The "LoRa GW node" is connected through an "AlLoRa Connector" to a VLC Access Point (AP), which is also embedded with a LoRa adapter interface. Specifically, the VLC AP has a double network interface for both LoRa and optical wireless communication links. Indeed, the VLC AP is connected in downlink to the PD node (*i.e.*, the receiver node), which is also equipped with a LoRa adapter (*i.e.*, the AlLoRa connector), which allows sending LoRa packets directly to the LoRa gateway through the AlLoRa connector laying in the VLC AP node. Notice that the LoRa connectivity links are bidirectional between the LoRa GW and the VLC AP, while only in uplink from the PD to the VLC AP. This allows one to send LoRa request packets from the PD to the VLC AP, which will redirect to the LoRa GW to take an action. The schematic in Fig. 1(*a*) can be easily extended into a point-to-multipoint topology as depicted in Fig. 1(*b*), where a single LoRa GW can control multiple VLC APs. This configuration depicts a branching topology, where the LoRa GW connects to two VLC APs in parallel, each connected to a PD node through a VLC interface and a VLC connector. Finally, Fig. 1(*c*) shows a mesh topology with overlapping point-to-multipoint links, where a single VLC AP can communicate to multiple PDs, and similarly a single PD can send LoRa request packets to multiple VLC APs. This configuration is applicable in crowded realistic scenarios, such as a shopping mall or a hospital.

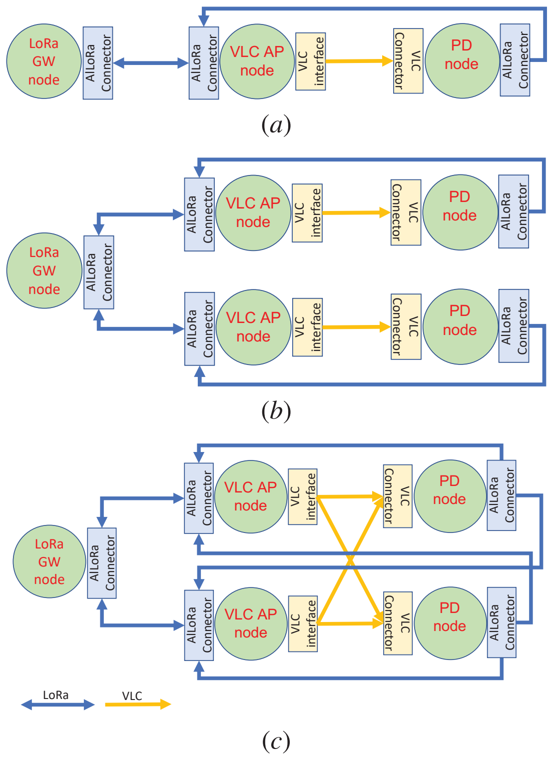

Fig. 1: Schematic of different communications modes in IRON framework, providing (*a*) point-to-point, (*b*) point-to-multipoint, and (*c*) overlapping point-to-multipoint connectivity. *Blue lines* represent the LoRa links, while *yellow lines* are downlink VLC links.

III. IRON Controlling function

Let us consider a VLC indoor system where a set of "white" light APs *i.e.*, $\mathcal{A} = \{a_1, a_2, \ldots, a_N\}$, are installed on the ceiling for illumination purpose. The VLC APs are embedded with the IRON protocol, and comprise a LED array with number of elements n_{LED}. A single LED emits the radiant intensity following the generalized Lambertian distribution. The DC gain of the Line of Sight VLC channel is given by

$$H(0) = \begin{cases} \frac{(m+1)A_{PD}}{2\pi d^2} \cos^m(\phi) T_s(\theta) g(\theta) \cos(\theta), & 0 \leq \theta \leq \phi_c \\ 0, & \theta \geq \phi_c \end{cases} \tag{1}$$

where A_{PD} [cm^2] is the surface area of the photodetector, ϕ is the irradiance angle, ϕ_c is the Field of View (FOV) of the receiver, and d [m] is the distance between the VLC AP and the PD. Also, $T_s(\theta)$ is the optical filter gain, and $g(\theta)$ is the optical concentrator gain, defined as $g(\theta) = n^2/\sin(\theta)$, with n as the refractive index and θ is the incidence angle. Finally, m is the Lambertian radiant order, expressed as $m = -\frac{\ln 2}{\ln \cos(\phi_{1/2})}$, with $\phi_{1/2}$ as the semi-angle of the LED at half power. From Eq. (1), the optical power received at the PD will be given by

$$P_{rx} = P_{LED} n_{LED}^2 H(0), \tag{2}$$

where P_{LED} [mW] is the power of a single LED and n_{LED} is the number of active LED array at the VLC AP.

An UE is moving in the room along a random path *i.e.*, $\mathcal{P} = \{p_1, p_2, \ldots, p_P\}$. In each position, the UE is expected to receive a given data rate that satisfies the user requirements *i.e.*, $\mathcal{R} = \{50, 70, 90, 110\}$ Mbps. Specifically, the following condition should be guaranteed *i.e.*,

$$\Theta_{p_i} \geq \mathcal{R}_j, \tag{3}$$

where Θ_{p_i} is the received data rate in the i-th UE position p_i, and j is the index of the user requirement. If Eq. (3) is not satisfied, the UE will notify the LoRa GW through the AlLoRa Connector, and will request to turn on a new VLC AP to increase the received data rate till reaching the user requirement. This occurs by transmitting an "`AP_ON`" LoRa packet, where the information about UE's position is shared.

Algorithm 1 represents how LoRa messages are exchanged in IRON framework. We assume that the payload of a LoRa packet is 14 byte long and contains the information related to the requests for (*i*) turning on a new AP and (*ii*) updating specific parameters for that AP recently activated. Specifically, we distinguish two procedures *i.e.*, (*i*) *check quality*, and (*ii*) *AP update*. The first procedure consists in assessing the data rate at the UE satisfies a given requirement as expressed in Eq. (3). The outcome of the quality check procedure is a Boolean variable, which will be 0 if Eq. (3) is satisfied.

We assume that the grid is made up of multiple APs and only those in the set $\mathcal{A}$ are on. The remaining APs are off and will be turned on apon receiving the "`AP_ON`" request. Specifically, the LoRa gateway will control the grid of APs and turn on a new AP that will be the one closer to the given position. Notice that transmission of an "`AP_ON`" message does not guarantee that the user requirement will be suddenly satisfied. Indeed, when a new AP is on, default parameters are assumed such as the number of LEDs comprising the AP (*i.e.*, n_{LED}), the bandwidth (*i.e.*, B), and the half power semi-angle (*i.e.*, $\phi_{1/2}$). In fact, if Eq. (3) is not satisfied after activation of a new VLC AP, the *AP update* procedure will be initiated. It consists in updating different VLC parameters following a given order. Initially, the "`UPDATE`(n_{LED})" LoRa packet will be sent to request of activating more LEDs at the AP recently on. If the quality check is still not guaranteed, then an "`UPDATE`(B)" LoRa packet will be sent with the request of increasing the LED bandwidth (*i.e.*, an increase of 1% is provided for each request received). Finally, if still the quality check fails, an "`UPDATE`(Ψ_{half})" LoRa packet will be sent to request of increasing the half power semi-angle of the LEDs (*i.e.*, an increase of 10° is provided for each request received till reaching a maximum value). Notice that after each LoRa request packet, the assessment of data rate requirement is provided.

Algorithm 1: IRON Message Exchange

Input: $\mathcal{P} = \{p_1, \ldots, p_i, \ldots, p_P\}$ ▷ Set of user positions along a random path
$\mathcal{A} = \{4, 6, 8\}$ ▷ Initial set of APs deployment
$\mathcal{R} = \{50, 70, 90, 110\}$ ▷ User requirement
$j = \{1, \ldots, 4\}$ ▷ Index of user requirement
$check = 0$ ▷ Quality check Boolean variable
Output: $\Theta_{\mathcal{P}}$ ▷ Achievable user data rate
n_{pkt} ▷ Number of LoRa packets

foreach $p_i \in \mathcal{P}$ **do**
  if $check = 0$ **then**
    Procedure `proc`(*check quality*)
      if $\Theta_{p_i} < \mathcal{R}_j$ **then**
        $check = 1$ ▷ Check positive
        send "`AP_ON`" packet
        $n_{pkt} \leftarrow n_{pkt} + 1$
        update Θ_{p_i}
      else
        $check = 0$ ▷ User quality satisfied
      return $check$
  else
    Procedure `proc`(*AP update*)
      send "`UPDATE`(n_{LED})" LoRa packet
      $n_{pkt} \leftarrow n_{pkt} + 1$
      update Θ_{p_i}
      if $\Theta_{p_i} < \mathcal{R}_j$ **then**
        $check = 1$
        send "`UPDATE`(B)" packet
        $n_{pkt} \leftarrow n_{pkt} + 1$
        update Θ_{p_i}
        if $\Theta_{p_i} < \mathcal{R}_j$ **then**
          $check = 1$
          send "`UPDATE`(Ψ_{half})" packet
          $n_{pkt} \leftarrow n_{pkt} + 1$
        else
          $check = 0$ ▷ User quality satisfied
      else
        $check = 0$ ▷ User quality satisfied
      return $check$

IV. Simulation results

We simulated a VLC indoor system *i.e.*, a $20 \times 20 \times 4$ m^3 open office, where $\mathcal{A} = \{4, 6, 8\}$ APs are deployed on the ceiling following either a grid or a random configuration. The UE is a PD embedded with IRON protocol, moving randomly within the room in each simulation run. The following VLC parameters are assumed in our simulations *i.e.*, the LED angle of irradiance ϕ is set to 70°, the PD FOV ϕ_c is 80°, the PD physical area is 1 cm^2, the communication bandwidth B is 1 MHz, the refractive index is 1.5, the optical filter gain is set to 1, the initial number of LEDs is 4, and the single LED power is set to 10 mW.

Fig. 2 depicts the average data rates at the UE, achieved through IRON protocol in each position of a random path and for different user requirements, assuming different VLC APs as initial network configuration. The user requirements are largely overcome especially for limited number of APs as initial network configuration. Indeed, 4 APs are not able to guarantee data rates higher than 50 Mbps in each position

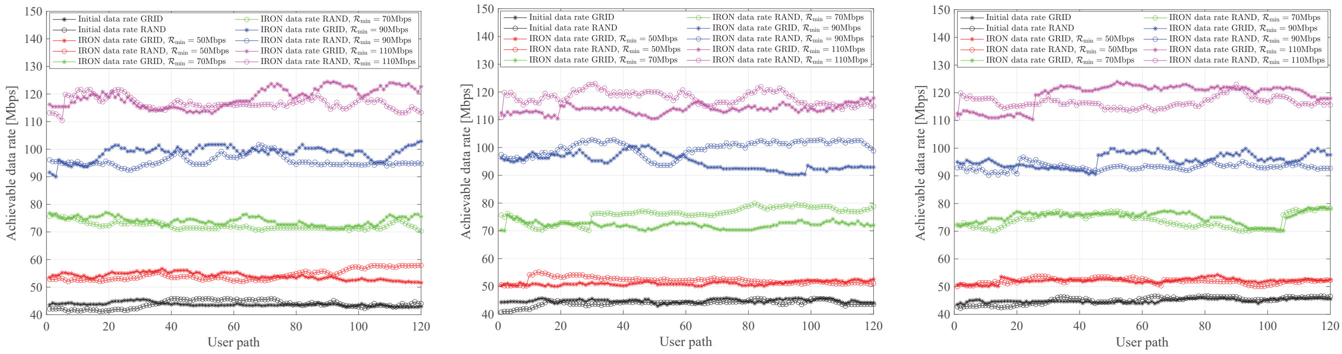

(a) (b) (c)

Fig. 2: Comparison of end user average data rates achieved along random paths (each comprised of 120 steps), in case of different quality requirements and assuming different initial network configurations *i.e.*, (a) 4, (b) 6, and (c) 8 VLC APs, following a grid and random deployment.

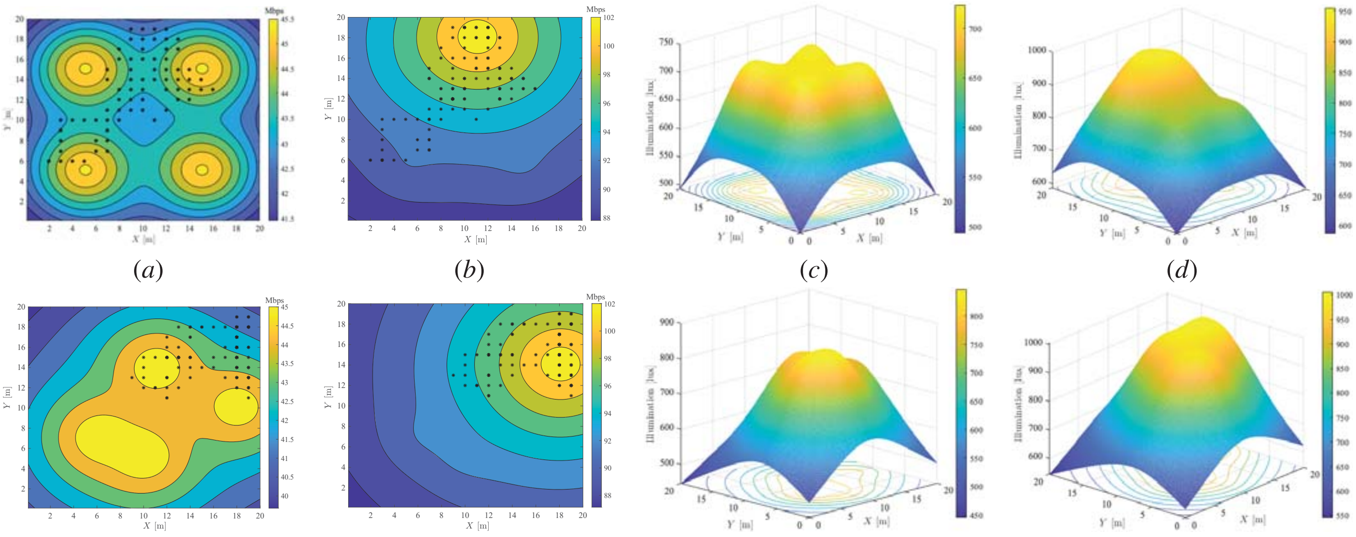

(a) (b) (c) (d)

(e) (f) (g) (h)

Fig. 3: Comparison of data rate and illumination distribution maps in an indoor environment comprised of 4 VLC APs as initial configuration deployed on a grid (*first row*) and randomly deployed (*second row*). Effect of IRON technique on (b-f) data rate and (d-h) illumination distribution to reach 90 Mbps. The UE's path is random in each simulation run and is marked with asterisks.

of a given user path. Turning a new AP on and updating its physical parameters allows to increase the end user data rate, which will result higher than the minimum user requirement.

The effect of different AP deployments on the achievable data rate is not particularly evident from Fig. 2, which shows the requirements are well overcome with both two configurations. In contrast, this effect is significant in Fig. 3 that shows the simulation results expressed as maps of data rate distribution, in case of a 4-APs network assumed as initial configuration, and for a user requirement of 90 Mbps. The grid deployment is easily noticed in Fig. 3(a). After the IRON approach, where new APs are activated, we observe that for the random deployment the data rate is higher in those positions of UE's path. On the other hand, for the grid deployment reported in Fig. 3(b), the data rate requirement is still guaranteed but reduced values are observed in some UE's positions. It is evident that the AP random deployment focuses the data rate distribution in those positions that need to reach the quality requirements, while the grid configuration is limited to the activation of APs in restricted positions. Similar considerations apply for the illumination distribution within the room, as depicted in Fig. 3(c-d) and (g-h). The IRON approach provides an increase of illumination, focused in specific positions in case of random deployment, while in the grid configuration illumination is smoother and not concentrated in specific positions. However, maximum allowed illumination is met to reduce eye safety issues.

The choice of AP deployment affects also the number of new VLC APs activated, as well as the number of LoRa packets, as depicted in Fig. 4. It is shown the overall number of new APs turned on to meet the user requirements, together with the number of LoRa packets shared to activate new APs or update specific VLC physical parameters. From Fig. 4(*a*) for a 4-APs network initial configuration, one more AP is needed to guarantee 50 Mbps along the user path, while 5 more APs are needed to achieve the same requirement in a 8-APs initial configuration. In general, more than two more APs, accordingly updated, are needed to guarantee quality requirements. Indeed, we observe an increasing number of LoRa packets requesting for AP updates that allow to meet the data rate constraints. On the other side, for reduced quality requirements (*i.e.*, 50 Mbps) a higher number of APs is needed as AP updates are not enough to meet the data rate constraints. In contrast, for the random deployment depicted in Fig. 4(*b*), the number of new APs activated to meet the use requirements is particularly small and limited to a maximum of two APs to reach 110 Mbps. Consequently, also the number of LoRa packets is reduced. This behavior is due to the random deployment of APs, which allows to activate new APs especially in those positions that need a data rate enhancement.

Notice that the exchange of LoRa packets affects the energy consumption of LoRa devices. Assuming each LoRa packet causes an energy consumption of 100 mW, we observe the energy consumption is limited to ≈ 2.5 Watt in a scenario with 10 VLC APs and 110 Mbps as minimum requirement.

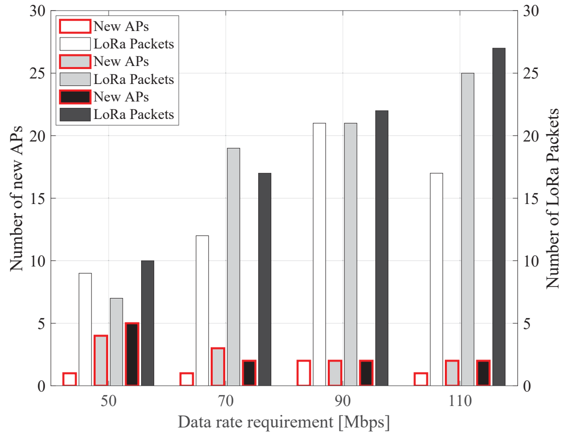

(*a*)

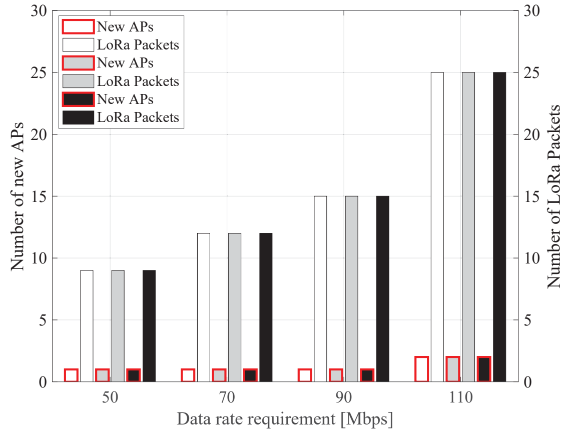

(*b*)

Fig. 4: Number of new APs added in the system (*red contour*) and the associated number of LoRa packets sent to the LoRa GW (*black contour*), needed to reach a given data rate requirement, in case of 4 (*white*), 6 (*gray*), 8 (*black*) APs as initial network configuration, for (*a*) grid; (*b*) random deployment.

V. Conclusions

This paper introduced IRON, a novel integrated LoRa-VLC system tailored for IoT applications. Unlike conventional RF-based IoT solutions, IRON capitalized on the broad spectrum of optical wireless technology to boost network performance, without impacting on the overall energy consumption. The unique IRON message exchange protocol was also detailed, enabling precise control over VLC connectivity links based on specific user requirements. This integration resulted in a highly controllable VLC system, efficiently managed through a LoRa GW subsystem, marking a significant advancement in the realm of IoT communication technologies.

Acknowledgment

This work has received funding from the Horizon 2020 research and innovation staff exchange grant agreement No 101086387. This article was based upon work from COST Action NEWFOCUS CA19111, supported by COST (European Cooperation in Science and Technology).

References

[1] S. Amendola, R. Lodato, S. Manzari, C. Occhiuzzi, and G. Marrocco, "RFID Technology for IoT-Based Personal Healthcare in Smart Spaces," *IEEE Internet of Things Journal*, vol. 1, no. 2, pp. 144–152, 2014.

[2] Y. C. Manie, C.-K. Yao, T.-Y. Yeh, Y.-C. Teng, and P.-C. Peng, "Laser-Based Optical Wireless Communications for Internet of Things (IoT) Application," *IEEE Internet of Things Journal*, vol. 9, no. 23, pp. 24 466–24 476, 2022.

[3] H. Larthani, A. Zrelli, and T. Ezzedine, "On The Detection of Disasters: Optical Sensors and IoT Technologies," in *2018 Intl. Conf. on Internet of Things, Embedded Systems and Communications*, 2018, pp. 142–146.

[4] M. Margarat, et al., "All Optical sensors for IOT applications," in *2020 Intl. Conf. on System, Computation, Automation and Networking*, 2020.

[5] F. Delgado-Rajo, et al., "Hybrid RF/VLC network architecture for the internet of things," *Sensors*, vol. 20, no. 2, 2020.

[6] V. Slany, et al., "New hybrid IoT LoRaWAN/IRC sensors: SMART water metering system," *Computers, Materials & Continua*, vol. 71, no. 3, pp. 5201–5217, 2022.

[7] A. I. Petrariu, A. Lavric, and E. Coca, "VLC for vehicular communications: A multiple input multiple output (MIMO) approach," in *2018 Intl. Conf. on Development and Application Systems (DAS)*, 2018.

[8] R. N. Gadens, A. de Almeida Prado Pohl, and P. de Tarso Neves, "The LoRa-Modulation Technique Applied to Outdoor Visible Light Communication Links," in *2021 SBFoton Intl. Optics and Photonics Conf. (SBFoton IOPC)*, 2021, pp. 1–4.

[9] B. A. Arratia Uribe, E. Rosas, C. T. Calafate, J.-C. Cano, J. Cecilia, and P. Manzoni, "AlLoRa: Empowering Environmental Intelligence Through an Advanced LoRa-Based IoT Solution," pp. 378–383, 2023.

[10] Borja Genoves Guzman, et al., "Prototyping Visible Light Communication for the Internet of Things Using OpenVLC," *IEEE Commun. Mag.*, vol. 61, no. 5, pp. 122–128, 2023.